

Ultrafast resonant optical scattering from single gold nanorods: Large nonlinearities and plasmon saturation

Matthew Pelton,* Mingzhao Liu, Sungnam Park, Norbert F. Scherer, and Philippe Guyot-Sionnest

*Department of Physics, Department of Chemistry, and James Franck Institute,
University of Chicago, 5640 S. Ellis Ave., Chicago, IL 60637*

(Dated: December 2, 2024)

We measure intensity-dependent changes in the nonlinear optical scattering from individual Au nanorods excited with ultrafast laser pulses at their plasmon resonance frequency. Isolating single rods allows the measurement of a greatly enhanced nonlinearity compared to nanorod ensembles or bulk Au. Surprisingly, the ultrafast nonlinearity can be attributed entirely to heating of conduction electrons and does not exhibit any coherent effect associated with plasmon oscillation. This suggests a previously unobserved damping of strongly driven plasmons.

PACS numbers: 78.67.Bf, 78.47.+p

Conventional photonic devices are restricted by the diffraction limit to be larger than half the optical wavelength, restricting the possibilities for miniaturization. One way to overcome this limit is to couple light to surface plasmons in metal nanostructures [1]. Preliminary steps have been made, for example, towards using surface plasmons in nanoparticles to construct sub-wavelength waveguides [2, 3]. Actively controlling light propagation in such structures will require an understanding of the ultrafast nonlinear response of the individual elements. Such an understanding is also crucial for the treatment of effects such as surface-enhanced Raman scattering [4, 5], since it may limit the magnitude of local electromagnetic fields that can be achieved in real structures.

Previous experiments have generally involved excitation of metal-nanoparticle ensembles at frequencies away from the plasmon resonance, and thus measure incoherent effects related to the heating of electrons [6, 7, 8, 9, 10, 11, 12]. Exciting and probing rods on resonance has the potential to reveal nonlinearities associated with the coherent oscillation of the plasmons themselves. Unfortunately, the optical response of the ensemble is broadened by the inhomogeneous distribution of particle sizes and shapes. The non-resonant particles have nonlinear responses much smaller than or even opposite in sign to the resonant particles, leading to an overall effect that is greatly reduced and whose dynamics are obscured. By contrast, isolating single particles allows the quantitative measurement of inherent nonlinearities [13, 14].

In this Letter, we report the first measurements of resonant nonlinearities of surface plasmons in single metal nanoparticles, specifically Au nanorods. We measure a nonlinear scattering cross-section that is much larger than that of nanorod ensembles or of bulk Au. Surprisingly, the measured effect can be explained entirely as the result of heating of conduction electrons. There is no apparent nonlinearity directly associated with plasmon oscillation, suggesting that the strong optical driving fields induce a novel damping and saturation of the plasmonic response.

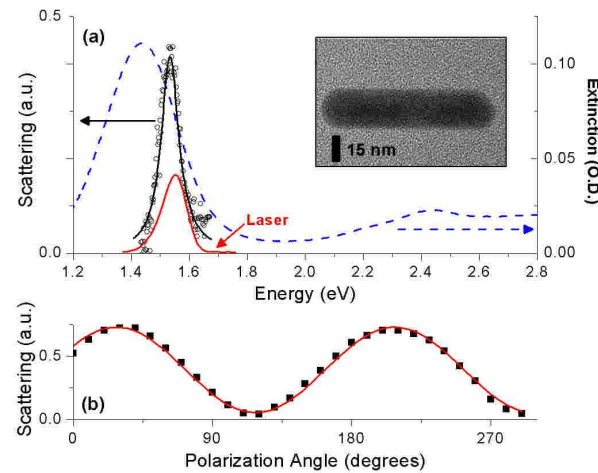


FIG. 1: (Color online) (a) Extinction of an ensemble of Au nanorods in aqueous solution (dashed blue line); scattering spectrum from a single nanorod on a glass surface (circles); calculated scattering spectrum for a single rod (solid black line); and measured spectrum of the laser used to excite the rods (solid red line). Inset: Au nanorod, on a carbon grid, imaged with a transmission-electron microscope (TEM). (b) Intensity of laser light scattered off a single rod as the incident laser polarization is varied (squares), and sinusoidal fit (red line).

The Au nanorods are chemically synthesized using a seed-mediated growth method [15, 16]; by controlling the growth conditions, this process can yield single-crystal rods with smooth surfaces, controllable aspect ratios, and nearly quantitative yield [17]. The rods exhibit a strong longitudinal plasmon resonance, whose frequency is determined by the aspect ratio of the rods [18]. Damping due to interband transitions is reduced by selecting particles with a plasmon resonance near 1.55 eV [19], which matches the Ti:Sapphire laser light used to excite and probe the rods.

The sample consists of sparsely dispersed and isolated rods, bound to a glass coverslip using a mercaptosilane coupling agent [20]. Atomic-force microscopy (AFM) is used to verify that over 75% of the rods are well isolated on the sample surface, with an average inter-rod spacing greater than 2 μm . Optical measurements on the single rods are made using total-internal-reflection microscopy [16, 17, 21]. Incident light is focussed onto the sample through a glass prism. Scattered light is collected using a microscope objective and is imaged onto a multimode optical fiber, which selects a 1.5 μm spot on the sample for observation. For spectral measurements, the light is sent to a spectrometer equipped with a cooled CCD array detector (Andor); for time-resolved measurements, the light is sent to an avalanche photodiode (Hamamatsu).

Single rods are identified by exciting with incoherent white light and measuring the scattering spectrum; a typical spectrum is shown in Fig. 1(a). The narrow peak compared to the ensemble indicates that the scattering comes from a single rod; this is further supported by the strong polarization dependence of the scattering, as shown in Fig. 1(b).

The scattering spectrum is quantitatively compared to a calculation in the quasi-static approximation [16, 17, 18], as shown in Fig. 1(a). We treat the rod as a prolate ellipsoid, and approximate the asymmetric environment of the rod as a homogeneous, transparent medium with dielectric constant 1.3. The imaginary part of the dielectric function of Au is taken to be [22, 23, 24]

$$\epsilon_2(\omega, T_e) = \frac{\omega_p^2 \gamma(T_e)}{\omega [\omega_p^2 + \gamma(T_e)^2]} + \epsilon_2^{d-c}(\omega, T_e), \quad (1)$$

where ω is the optical frequency and T_e is the temperature of the conduction electrons in the rod. The first term is the Drude free-electron contribution; ω_p is the bulk plasmon frequency, and γ is the plasmon damping rate. The second term is the contribution of transitions between the d and the conduction bands. The real part of the dielectric function is calculated from this imaginary part using the Kramers-Kronig relation. The matrix elements of the interband transitions and the Drude plasmon frequency are adjusted to reproduce experimental dielectric functions [25]. The only free parameter is the aspect ratio of the rod; for this rod, the fitted aspect ratio is 5.25, consistent with the rod shapes measured by TEM. (See inset of Fig. 1(a)). A different choice of refractive index for the surrounding medium changes the fitted nanorod aspect ratio, but has no other appreciable effect.

Nonlinearities of the single nanorods are measured using an interferometric scattering technique. The rods are excited with 20-fs pulses from a mode-locked, cavity-dumped Ti:Sapphire laser [26]. The pulses are split into two equal-intensity parts [14, 27], and the delay of one of the pulses is controlled relative to the other by moving

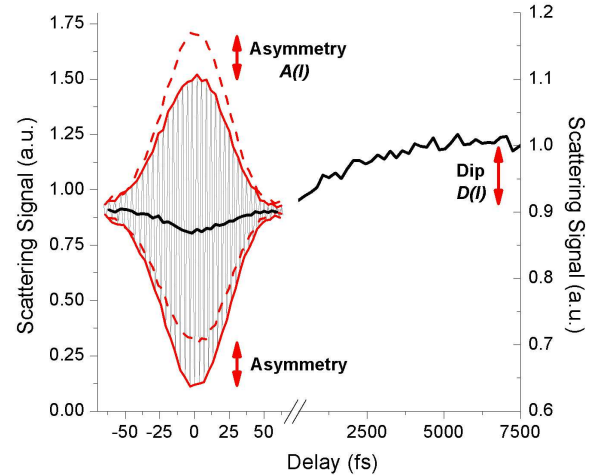


FIG. 2: (Color online) Single-rod scattering signal as a function of delay between two incident laser pulses. Left-hand side: scattering intensity for overlapping pulses with an energy of 47 pJ (light line); envelope of the interference pattern (solid red line); the same envelope, inverted about the average scattering signal at a delay of 75 fs (dashed red line); and the average of the upper and lower envelopes (heavy line). Right-hand side: scattering intensity for non-overlapping pulses with an energy of 94 pJ. Note that both vertical and horizontal scales are different on the two sides of the graph.

a retroreflector, using either a calibrated stepper motor or a piezoelectric transducer. A single lens focuses the two pulses to a common 20- μm spot on the sample. The signal is processed by a lock-in amplifier, which is synchronized to a chopper that modulates both laser beams.

Fig. 2 shows an example of an interference pattern traced out by the measured scattering signal for short delays; this pattern exhibits a pronounced asymmetry in intensity. When the laser pulses interfere constructively, the incident intensity is doubled, but the amount of scattering from the rod increases by less than a factor of two, showing that the scattering cross-section of the rod is lower for the higher intensity. The interference patterns do not change as the repetition rate of the laser is varied, indicating that slow, cumulative effects are not important. The nonlinearity thus arises within the 20-fs pulse duration.

These measurements make it possible to establish the magnitude of the ultrafast nonlinearity. Figure 3(a) shows the measured asymmetry *vs.* the laser intensity, I , for three different rods. The linear dependence indicates a third-order nonlinearity; that is, the scattering cross-section is $\sigma(I) = \sigma^{(0)} + I\sigma^{(3)}$, with a normalized nonlinear cross-section $\sigma^{(3)}/\sigma^{(0)} = (7.5 \pm 0.9) \times 10^{-11} \text{ cm}^2/\text{W}$. Transient-transmission measurements on nanorod ensembles in solution show a corresponding av-

verage nonlinear cross-section of approximately 2.5×10^{-13} cm²/W [28]; the significantly lower value is the result of the large number of non-resonant nanorods, which can have nonlinearities opposing those of the resonant rods. The single-rod nonlinear cross-section implies a nonlinear susceptibility for Au over the laser bandwidth of $\chi^{(3)} \approx 5 \times 10^{-18}$ m²/V². This is between one and two orders of magnitude larger than the $\chi^{(3)}$ of bulk Au [29], consistent with the local field confinement in the Au rods. As a result of this large nonlinearity, the change in scattering cross-section can reach over 20% at high laser intensities. If the laser power is increased further, optical damage occurs, and the scattering signal gradually and irreversibly decreases.

Further insight into the measured nonlinearity is obtained by measuring the dependence of the nanorod scattering spectrum on incident laser power. Results for a particular nanorod are shown in Fig. 3(b); an intensity-dependent red shift $\Delta\omega$ and line broadening $\Delta\gamma$ are clearly seen. Both effects are linear in I ; for this rod, $\Delta\omega = 59$ meV/nJ, and $\Delta\gamma = 87$ meV/nJ.

Having established the magnitude of the nonlinearity, we next investigate its time dependence. We perform measurements with longer time delays, so that the two laser pulses no longer overlap. Figure 2 shows a representative result, and Fig. 3(c) gives similar results for different laser powers. The response is characteristic of the heating of conduction electrons by the laser pulse, followed by their cooling and equilibration with lattice phonons [7, 8, 9, 28]. Increasing the delay up to 150 ps results in no detectable change in the scattering signal, indicating that effects related to the heating of lattice phonons are unimportant on experimental time scales. The reported data have been normalized to the signal at long delays; any ultrafast nonlinearity arising within the laser pulse duration will result in a change in this reference level, but will not otherwise not affect the delay-dependent data.

The picosecond-scale results can be modeled as follows. The amount of light transferred from the first laser pulse to the conduction electrons is determined by calculating the nanorod absorption cross-section; this energy transfer results in a higher electron temperature, T_e . The subsequent evolution of T_e is calculated by treating the conduction electrons and the lattice phonons as two coupled thermal reservoirs [10, 28]. The effect of elevated T_e is to alter the dielectric function for Au, as described by Eqn. (1). The primary contribution is an increase in interband transitions due to the broadening of the conduction-electron distribution near the Fermi level [22, 23, 24]. The changes in the dielectric function cause the plasmon resonance to broaden and shift, and the modified plasmon resonance determines the amount of light scattered from the second laser pulse. This calculated scattering signal is fit to the data using a single free parameter, relating the measured laser power to the opti-

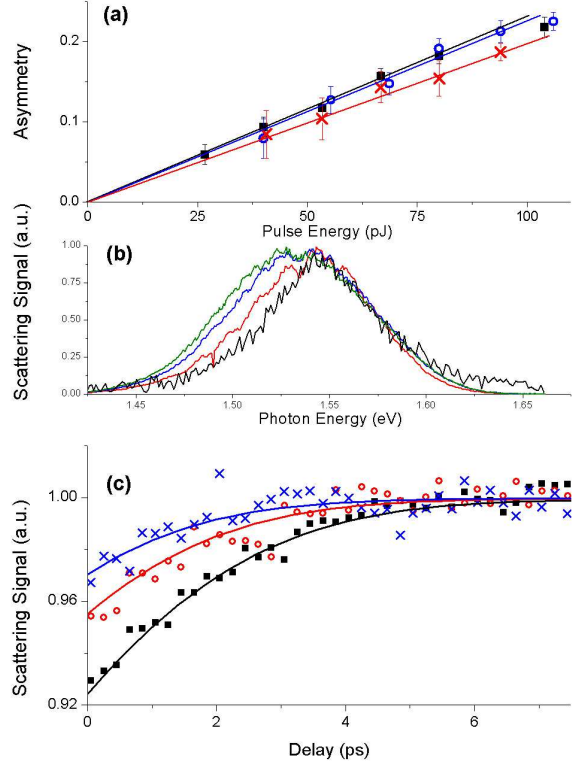


FIG. 3: (Color online) (a) Measured asymmetry in interference patterns for three different rods. (b) Normalized single-rod scattering spectra for different incident intensities. The rightmost curve is the linear spectrum measured using incoherent, broadband excitation. The other curves are measured using a single laser beam, and correspond to pulse energies of 82, 192, and 220 pJ, from right to left. (c) Measured single-rod scattering signal as a function of time delay between two incident laser pulses, normalized by the measured signal at a delay of 20 ps (points); calculated change in scattering (lines). The three curves, from top to bottom, correspond to pulse energies of 26, 53, and 94 pJ.

cal intensity incident on the rod. Fig. 3(c) shows results for three different laser powers from a single rod; equally good agreement was obtained for several other laser powers and for other rods, indicating that electron heating can account for the measured nonlinearity on picosecond time scales.

Unexpectedly, the same model also quantitatively explains the measured nonlinearities on femtosecond time scales. More precisely, we can extrapolate the measured thermal nonlinearity for a given laser intensity, I , to zero time delay; this gives a “dip” $D(I)$ in the normalized scattering signal. (See Fig. 2.) The measured values of $D(I)$ can be compared to the asymmetries, $A(I)$, of the measured interference patterns. Assuming that the only nonlinearity, even for the shortest time delays, is due to

electron heating, we obtain $A(I) = 2D(2I)$ (taking into account the dependence of the reference level for $D(I)$ on the intensity of the two laser pulses). We observe exactly this relationship within our experimental error, meaning that we see no change in the dynamics of the nonlinearity as we move from femtosecond to picosecond time scales.

This strongly suggests that a nearly thermal distribution of electrons is produced in the rod within a time short compared to the 20-fs laser pulse duration. This is unexpected, since the resonant laser pulses should excite plasmons that remain coherent for 15 fs. Any initial nonlinearity would then be due to deviation of the plasmon motion from perfect harmonic oscillation, due, for example, to the confinement of electrons by the boundaries of the rod [30, 31]. The apparent absence of any such coherent nonlinearity, and the immediate emergence of an incoherent thermal nonlinearity, indicate that the coherence of the plasmon is destroyed by the strong, resonant laser excitation. As shown in Fig. 3(b), the plasmon experiences increased damping at high laser powers; the plasmon lifetime then becomes short compared to the pulse duration, making it impossible to resolve any coherent plasmonic nonlinearities. The increased damping may be due to a greater rate of dephasing collisions with the nanorod boundaries or to higher-order plasmon-plasmon or plasmon-electron interactions. Such interactions may also be involved in the significant redistribution of electron energies that has been observed in photoemission experiments [32].

The measurements described in this Letter have established for the first time the magnitude of resonant optical nonlinearities in single Au nanorods. A benchmark value of 20% has been obtained for the nonlinear change in the scattering cross-section, using pulse energies that introduce no optical damage. Surprisingly, resonant excitation of plasmons results in the same nonlinearity as incoherent excitation of conduction electrons. This indicates that strongly driven plasmons experience a new, intensity-dependent damping. There are still several potential routes towards achieving stronger nonlinearities in these systems, such as embedding the nanorods in a polarizable medium, or assembling them into ordered structures. Our current observations thus represent a first step towards achieving very large optical nonlinearities on the nanometer scale, but also point out the new issue of plasmon damping and saturation under strong excitation.

We thank Dr. A. Bakhtyari for valuable assistance and Prof. H. Petek for helpful discussions. This work was principally supported by the MRSEC program of the NSF under grant No. DMR 0213745, with additional support from the UC-ANL Consortium for Nanoscience Research and from NSF grant No. CHE 0317009. M.P. is supported by the Grainger Postdoctoral Fellowship in Experimental Physics from the University of Chicago.

* Electronic address: pelton@uchicago.edu

- [1] W. L. Barnes, A. Dereux, and T. W. Ebbesen, *Nature* **424**, 824 (2003).
- [2] M. Quinten, A. Leitner, J. R. Krenn, and F. R. Aussenegg, *Opt. Lett.* **23**, 1331 (1998).
- [3] S. A. Maier *et al.*, *Nature Materials* **2**, 229 (2003).
- [4] S. Nie and S. R. Emory, *Science* **275**, 1102 (1997).
- [5] K. Kneipp *et al.*, *Phys. Rev. Lett.* **78**, 1667 (1997).
- [6] M. J. Feldstein *et al.*, *J. Am. Chem. Soc.* **119**, 6638 (1997).
- [7] J. H. Hodak, A. Henglein, and G. V. Hartland, *J. Phys. Chem. B* **104**, 9954 (2000).
- [8] C. Voisin, N. D. Fatti, D. Christofilos, and F. Vallée, *J. Phys. Chem. B* **105**, 2264 (2001).
- [9] S. Link and M. El-Sayed, *Annu. Rev. Phys. Chem.* **54**, 331 (2003).
- [10] A. Arbouet *et al.*, *Phys. Rev. Lett.* **90**, 177401 (2003).
- [11] S. Link *et al.*, *Phys. Rev. B* **61**, 6086 (2000).
- [12] M. Hu *et al.*, *J. Am. Chem. Soc.* **125**, 14925 (2003).
- [13] T. Itoh, T. Asahi, and H. Masuhara, *Appl. Phys. Lett.* **79**, 1667 (2001).
- [14] Y.-H. Liau, A. N. Unterreiner, Q. Chang, and N. F. Scherer, *J. Phys. Chem. B* **105**, 2135 (2001).
- [15] B. Nikoobakht and M. A. El-Sayed, *Chem. Mater.* **15**, 1957 (2003).
- [16] M. Liu and P. Guyot-Sionnest, *J. Phys. Chem. B* **108**, 5882 (2004).
- [17] M. Liu and P. Guyot-Sionnest, *J. Phys. Chem. B* **109**, 22192 (2005).
- [18] C. F. Bohren and D. R. Huffman, *Absorption and Scattering of Light by Small Particles* (John Wiley & Sons, New York, 1983).
- [19] C. Sönnichsen *et al.*, *Phys. Rev. Lett.* **88**, 077402 (2002).
- [20] H. Jung *et al.*, *Nano Lett.* **4**, 2171 (2004).
- [21] C. Sönnichsen *et al.*, *Appl. Phys. Lett.* **77**, 2949 (2000).
- [22] R. Rosei, F. Antonangeli, and U. M. Grassano, *Surf. Sci.* **37**, 689 (1973).
- [23] R. Rosei, *Phys. Rev. B* **10**, 474 (1974).
- [24] M. Guerrisi, R. Rosei, and P. Winsemius, *Phys. Rev. B* **12**, 557 (1975).
- [25] P. B. Johnson and R. W. Christy, *Phys. Rev. B* **6**, 4370 (1972).
- [26] Y.-H. Liau, A. N. Unterreiner, D. C. Arnett, and N. F. Scherer, *Appl. Opt.* **38**, 7386 (1999).
- [27] H. Petek and S. Ogawa, *Prog. Surf. Sci.* **56**, 239 (1998).
- [28] S. Park, M. Pelton, M. Liu, P. Guyot-Sionnest, and N. Scherer, in preparation.
- [29] W. K. Burns and N. Bloembergen, *Phys. Rev. B* **4**, 3437 (1971).
- [30] M. Lippitz, M. A. van Dijk, and M. Orrit, *Nano. Lett.* **5**, 799 (2005).
- [31] The dipole moment induced by the applied field is equal to the product of the polarizability and the applied field, and is also equal to the number of electrons in the rod times their displacement times the electron charge. Using known material parameters for Au gives, for pulse energies of 100 pJ, an electron displacement approximately 8% of the rod length.
- [32] G. Banfi, G. Ferrini, M. Peloi, and F. Parmigiani, *Phys. Rev. B* **67**, 035428 (2003).